Adaptive Correction Method for an OCXO and Investigation of Analytical Cumulative Time Error Upperbound

Hui Zhou, Thomas Kunz, Howard Schwartz

Abstract

Traditional oscillators used in timing modules of CDMA and WiMAX base stations are large and expensive. Applying cheaper and smaller, albeit more inaccurate, oscillators in timing modules is an interesting research challenge. An adaptive control algorithm is presented to enhance the oscillators to meet the requirements of base stations during holdover mode. An oscillator frequency stability model is developed for the adaptive control algorithm. This model takes into account the control loop which creates the correction signal when the timing module is in locked mode. A Recursive Prediction Error Method is used to identify the system model parameters. Simulation results show that an oscillator enhanced by our adaptive control algorithm improves the oscillator performance significantly, compared to uncorrected oscillators. Our results also show the benefit of explicitly modeling the control loop. Finally, the cumulative time error upperbound of such enhanced oscillators is investigated analytically and comparison results between the analytical and simulated upperbound are provided. The results show that the analytical upperbound can serve as a practical guide for system designers.

1. Introduction

The timing module accuracy is crucial to the normal operation of WiMAX and CDMA base transceiver stations. Generally, the timing module on the base station is phase locked by a pulse per second (1pps) signal from GPS (Global Positioning System) satellites. Once GPS signals are lost and the timing module enters holdover mode, the accuracy of the timing module is dependent on the local oscillator. The 3GPP2 recommended that CDMA systems must not exceed 10 μs cumulative time error (CTE) for a period of no less than 8 hours in holdover mode [1]. WiMAX systems do not have a standard but a cumulative time error not exceeding 25 μs for a period of 8 hours in holdover mode is a target [2].

The time error Δt and the time duration T for which the frequency stability error is maintained are related to the stability of the oscillator $\Delta f/f_0$ through Equation (1). The term f_0 is the nominal frequency and the term Δf is the frequency error.

$$\frac{\Delta t}{T} = \frac{\Delta f}{f_0} \tag{1}$$

Applying Equation (1) to the CDMA cumulative time error of 10 μs over an 8 hour period in holdover mode, one can derive a maximum allowable frequency error of the oscillator of 0.35 ppb (parts per billion). A Double Oven Controlled Crystal Oscillator (DOCXO) is needed to meet the stability requirement over the 75 ℃ operation temperature range. The cost, size, and power consumption of a DOCXO increase as the frequency stability requirement rises. It is feasible to change this trend by using an adaptive model of the timing module during the locked mode and then using the resulting model to correct the oscillator frequency drift during holdover mode.

This paper shows that a single oven controlled crystal oscillator (OCXO) can be used in the timing module. A Recursive Prediction Error Method (RPEM) is used to develop an adaptive control approach to compensate the OCXO. Using an OCXO in the timing module, the physical size and power consumption of the timing module are reduced. The resulting timing module can be integrated onto the base station modem card and the cost is further reduced.

The paper also investigates the analytical cumulative time error upperbound of the timing module. This upperbound represents the performance bound of the timing module and determines the application range.

The remainder of this paper is organized as follows: Section 2 describes the background information about oscillators, key factors affecting oscillator frequency stability, and related work on enhancing oscillator precision. Section 3 describes the timing module system in the base station and the digital control loop which creates the correction signal in locked mode. Section 4 describes the adaptive control algorithm. In Section 5 the analytical CTE upperbound is investigated and Section 6 concludes the paper.

2. Background

Crystal oscillators are electronic circuits which use the mechanical resonance of vibrating crystals of piezoelectric materials to create periodically varying electrical signals. Crystal oscillators provide relatively accurate time and are the sources of relatively precise frequency. The frequency stability, low cost and small size of crystal oscillators have resulted in their ubiquitous usage as a frequency reference in electronic equipment. Crystal oscillators as frequency sources and frequency control components are widely used in the time and frequency research and production fields, such as the IT Industry, Communications, Electronic Instruments, Applied Electronic Techniques, Measurements, Aerospace Systems, Military Industry, etc.

Temperature is a first-order factor which affects the frequency stability of crystal oscillators. In general, oscillator frequency stability exhibits cubic dependence on temperature. However, quadratic temperature dependence is often enough to create an oscillator temperature-stability model when the temperature is around the turnover point of the crystal.

Ageing is another significant factor affecting frequency stability. Generally the ageing effect is not linear. However, when the ageing effect is considered over a short period of time, such as 24 hours, ageing can be considered as having a linear effect on frequency stability.

Some researchers have developed adaptive control algorithms for oscillators to enhance the oscillator frequency stability based on a correction signal. In [4], the authors developed an algorithm for performing adaptive temperature and ageing compensation of oscillators. The performance of the algorithm is evaluated based on experiments using a TCXO, an OCXO, and a Rubidium oscillator. The algorithm improves the performance of all of these oscillators in holdover mode. However, [4] did not analyze the characteristics of the correction signal, and therefore the model does not reflect the correction circuitry of the system. In [5] and [6], the authors used the Kalman Filter method to develop algorithms for enhancing the oscillator stability in holdover mode. These algorithms compensate the ageing effect of oscillators over a long period of time. In these works, the researchers did not compensate for the temperature effect. The authors in [7] used the Kalman Filter method to develop an algorithm to compensate for the ageing and temperature effect. The work in [2] used the Batch Least Squares method to compensate for the temperature effect. The algorithms developed in [7] and [2] assume a linear temperature dependency of the oscillators.

Our work in this paper has some distinct features and advantages. First, a quadratic temperature and frequency stability relation is included and the ageing effect is considered as well in a single model. Second, the effect of the control loop on creating the correction signal is included. The effect of the control loop will be discussed later in the paper. Third, we provide an analytical upperbound for the system performance which is not investigated by other researchers. Our work is based on simulation results and Matlab is used as the simulation platform.

3. Timing Module System and Digital Control Loop

The detailed system structure block diagram of the base station timing module is shown in Figure 1.The GPS receiver module offers a 1pps reference signal, which is coming from GPS satellites. Because all GPS satellites are equipped with ultra-high accurate rubidium atomic clocks, this 1pps reference signal is very precise. The stability of the GPS 1pps signal is not that high compared to its accuracy. Typically, the GPS receivers add a GPS noise ranging from 20ns to 30 ns rms (root mean square) jitter on the 1pps edge.

The complete digital control loop includes the digital phase detector, correction signal calculator, and the adaptive oscillator model. All of these functional models are resident on a Field Programmable Gate Array (FPGA), which includes a processor. A frequency source which is generated from the frequency multiplier is used to count the time interval between the rising edges of the 1pps reference signal from the GPS receiver module. A 10MHz OCXO is used to feed this frequency multiplier. The digital phase detector counts the numbers of periods of the frequency source. According to the count value, the correction signal is computed by the correction signal calculator. This correction signal is applied to a Digital to Analog Converter (DAC) to control the 10 MHz OCXO and it is also used to feed the adaptive oscillator model which can be used when the system loses the GPS signal. A temperature sensor is used to collect the ambient temperature.

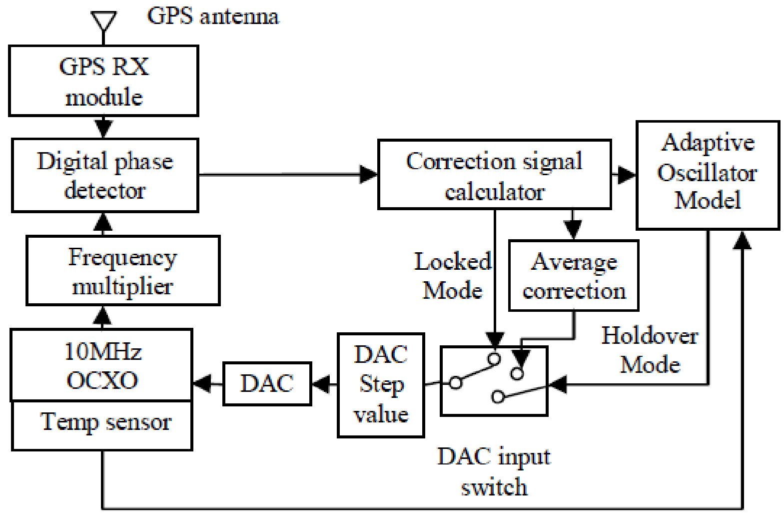

Figure 1. Detailed Block Diagram of the Timing Module System [2]

The 10MHz OCXO is the key component of the timing module, which is locked to the GPS reference signal through the control loop in the locked mode. In the holdover mode, the adaptive oscillator model creates the correction signal to the OCXO.

The accuracy of the OCXO is mainly dependent on temperature and ageing. The correction signal generated by the control loop compensates for the effect of these factors on the accuracy of the OCXO. The OCXO frequency control signal is created by counting between adjacent rising edges of the GPS 1pps (pulse per second) signal. When the OCXO has no frequency drift, the count value is equal to the frequency of the frequency multiplier output +/- the error counts. These error counts represent the GPS noise.

When the OCXO experiences frequency drift, this drift appears as a bias on the mean count value. A moving average filter is used by the control loop to divide the OCXO frequency drift from the GPS noise. The error counts are multiplied by the digital phase detector resolution to produce the time error between the OCXO and the received GPS 1pps signal. All time errors are integrated to create the cumulative time error (CTE). CTE can be recursively calculated through Equation (2).

$$CTE_k = CTE_{k-1} + \beta \times error\ count \qquad (2)$$

The term β represents the digital phase detector resolution. The correction signal is created by combining the CTE and a moving average of the former correction signals.

$$correct = correct_{ref} - CTE_k/damp \qquad (3)$$

The term $correct_{ref}$ is the average of the last N correction signals. The term $damp$ is a constant which suppresses the GPS noise. A digital to analog converter (DAC) is used to convert the digital correction signal into an analog tuning voltage. The whole process of determining the tuning voltage follows these steps: first, the correction signal, which is digital and expressed in ppb (parts per billion), is divided by the OCXO tuning sensitivity (Kvco), which is expressed in ppb/volt. Therefore, the voltage which is applied to the tuning port of the OCXO is obtained. Second, the tuning voltage is divided by the DAC resolution, which is the ratio of the control voltage range to the total number of DAC steps. Thus the actual number of DAC steps is obtained, which is a binary word. The calculation of the DAC steps is:

$$DAC_{steps} = fix\left(\frac{correction\ signal}{Kvco * DAC_{resolution}}\right) \qquad (4)$$

The operator $fix(\cdot)$ truncates the arguments in the brackets toward zero. This DAC step value is fed into the DAC to obtain the real control voltage.

4. The Adaptive Control Algorithm

The OCXO frequency stability is dependent on ageing and ambient temperature. The oscillator frequency stability model is shown in Equation (5).

$$Osc_{stab}(k) = a \cdot u^2(k) + b \cdot u(k) + c + d \cdot k \qquad (5)$$

The term $Osc_{stab}(k)$ represents the oscillator frequency stability and its unit is ppb. The term $u(k)$ represents the ambient temperature. The terms a and b are coefficients of the temperature. The term c represents a non-zero initial offset. The term d is the ageing rate. The task of the adaptive control algorithm is to identify parameters a, b, c, and d while in locked mode and to create the correction signal to compensate for the oscillator frequency error while in holdover mode.

The correction signal equation is based on the digital control loop described in Section 3.

$$y(k) = \left(\frac{1}{2000}\right) * \sum_{t=k-2000}^{k-1} y(t) - \left(\frac{1}{150}\right) * \sum_{t=0}^{k-1}\{6.25 * fix[(v(t+1) - v(t) + a * u^2(t+1) + b * u(t+1) + c + d * (t+1) + 0.0229 * fix\left(\frac{y(t)}{0.0229}\right))/6.25]\} \quad (6)$$

In Equation (6), the term $y(k)$ represents the correction signal. The term $\left(\frac{1}{2000}\right) * \sum_{t=k-2000}^{k-1} y(t)$ represents $correct_{ref}$ in Section 3 and is the average of the last 2000 correction signals. The *damp* term in Section 3 is set to be 150. The value 6.25 is the digital phase detector resolution and its unit is *ns*. The term $6.25 * fix(\frac{\cdot}{6.25})$ guarantees that the resulting value is a multiple of 6.25. The value 0.0229 corresponds to the DAC resolution and $0.0229 * fix(\frac{y(t)}{0.0229})$ guarantees that the correction signal is a multiple of 0.0229 ppb.

The measurement noise is $v(t+1) - v(t)$. The reason for choosing $v(t+1) - v(t)$ rather than $v(t+1)$ is as follows. The measurement noise of the system comes from the GPS noise jitter. The GPS receiver receives the GPS 1 pulse per second (pps) signal. If there is no GPS noise jitter, the distance between GPS pulses should be exactly 1 second. However, GPS noise always exists and the distortion of the jitter has to be added into the distance between pulses. For example, if both the first and second GPS 1 pps signals are distorted by a +10 *ns* jitter, both the first and second pulse edges move +10 *ns*. Then the distance between two pulse edges is still 1 second. The perceived measurement noise is 0 ns. If the first 1 pps signal is distorted by a +10 ns jitter and the second 1 pps signal is distorted by a -10 ns jitter, the first edge moves +10 ns and the second edge moves -10 ns. The distance between two pulse edges is 1 second minus 20 ns. The perceived measurement noise in this case is -20 ns. Hence, the measurement noise is given by $v(t+1) - v(t)$.

Equation (6) has to be rearranged to apply the system identification algorithm to identify parameters *a*, *b*, *c*, and *d*. We set

$$Y1(k) = (-150) * y(k) + \left(\frac{150}{2000}\right) * \sum_{t=k-2000}^{k-1} y(t) \quad (7)$$

According to (6),

$$(-150) * y(k) = \left(-\frac{150}{2000}\right) \sum_{t=k-2000}^{k-1} y(t) + \sum_{t=0}^{k-1}\{6.25 * fix[(v(t+1) - v(t) + a * u^2(t+1) + b * u(t+1) + c + d * (t+1) + 0.0229 * fix(\frac{y(t)}{0.0229}))/6.25]\} \quad (8)$$

Hence,

$$(-150) * y(k) + \left(\frac{150}{2000}\right) * \sum_{t=k-2000}^{k-1} y(t) = \sum_{t=0}^{k-1}\{6.25 * fix[(v(t+1) - v(t) + a * u^2(t+1) + b * u(t+1) + c + d * (t+1) + 0.0229 * fix(\frac{y(t)}{0.0229}))/6.25]\} \quad (9)$$

Hence,

$$Y1(k) = \sum_{t=0}^{k-1}\{6.25 * fix[(v(t+1) - v(t) + a * u^2(t+1) + b * u(t+1) + c + d * (t+1) + 0.0229 * fix(\frac{y(t)}{0.0229}))/6.25]\} \quad (10)$$

The $\sum$ in Equation (10) can be removed by calculating the difference between $Y1(k)$ and $Y1(k-1)$.

$$Y2(k) = Y1(k) - Y1(k-1) = 6.25 * fix[(v(k) - v(k-1) + a * u^2(k) + b * u(k) + c + d * k + 0.0229 * fix(\frac{y(k-1)}{0.0229}))/6.25] \quad (11)$$

We introduce

$$B(k-1) = 0.0229 * fix(\frac{y(k-1)}{0.0229}) \quad (12)$$

So,

$$Y2(k) = 6.25 * fix((v(k) - v(k-1) + a * u^2(k) + b * u(k) + c + d * k + B(k-1))/6.25)$$
$$= v(k) - v(k-1) + a * u^2(k) + b * u(k) + c + d * k + B(k-1) + 6.25 * fix((v(k) - v(k-1) + a * u^2(k) + b * u(k) + c + d * k + B(k-1))/6.25) - [v(k) - v(k-1) + a * u^2(k) + b * u(k) + c + d * k + B(k-1)] \quad (13)$$

We introduce

$$\delta Y2(k) = 6.25 * fix(v(k) - v(k-1) + a * u^2(\text{k}) + b * u(k) + c + d * k + B(k-1)/6.25) - [v(k) - v(k-1) + a * u^2(k) + b * u(k) + c + d * k + B(k-1)] \quad (14)$$

So,

$$Y2(k) = v(k) - v(k-1) + a * u^2(k) + b * u(k) + c + d * k + B(k-1) + \delta Y2(k) \quad (15)$$

We define $Y3(k)$ as the difference between $Y2(k)$ and $B(k-1)$.

$$Y3(k) = Y2(k) - B(k-1)$$
$$= v(k) - v(k-1) + a * u^2(k) + b * u(k) + c + d * k + \delta Y2(k) \quad (16)$$

The term $\delta Y2(k)$ represents the quantization error caused by the digital phase detector resolution. This error is limited between -6.25ns and +6.25ns.

Equation (16) is an ARMAX model except for the inclusion of a quantization error $\delta Y2(k)$. The standard ARMAX model is shown in Equation (17).

$$Y3(k) = a * u^2(k) + b * u(k) + c + d * k + v(k) + e * v(k-1) \quad (17)$$

The term e is the coefficient of GPS noise received in last second. From Equation (16), e should be -1. However, the quantization error $\delta Y2(k)$ causes e to be close to, but not exactly, -1. Hence, we use $e * v(k-1)$ to represent $\delta Y2(k) - v(k-1)$. Thus, Equation (17) can be solved by the Recursive Prediction Error Method [3]. After parameter estimates are calculated, the estimated $\hat{Y}3(k)$ in holdover mode is obtained as

$$\hat{Y}3(k) = \hat{a} * u^2(k) + \hat{b} * u(k) + \hat{c} + \hat{d} * k \quad (18)$$

Hence, the estimated correction signal $\hat{y}(k)$ in holdover mode is calculated as Equation (19) according to Equation (6).

$$\hat{y}(k) = \left(\frac{1}{2000}\right) * \sum_{t=k-2000}^{k-1} \hat{y}(t) - \left(\frac{1}{150}\right) * \sum_{t=0}^{k-1}\{6.25 * fix[(\hat{Y}3(t+1) + 0.0229 * fix(\frac{\hat{y}(t)}{0.0229}))/6.25]\} \quad (19)$$

The ambient temperature profile is fixed and shown in Figure 2. The range of temperature variation in Figure 2 is 60℃. The cycle of temperature variation is 8 hours. This temperature range is large enough to represent the real working environment, although the operation temperature range is 75℃. The 8 hours cycle guarantees that we obtain the simulation results fast enough. For illustrating the performance of a corrected OCXO, 100 simulations are run and the maximum CTE is shown in Figure 3. The CTE for the uncorrected OCXO is also shown in Figure 3 as a comparison. The timing modules are in locked mode for 6 hours and then in holdover for 8 hours.

The simulation results indicate that the adaptive control algorithm provides a 100 fold improvement in the cumulative time error over the uncorrected oscillator. There is a sharp spike in corrected OCXO figure when training process just starts. The reason is that a non-zero initial offset exists in the system model and it does not affect the CTE improvement.

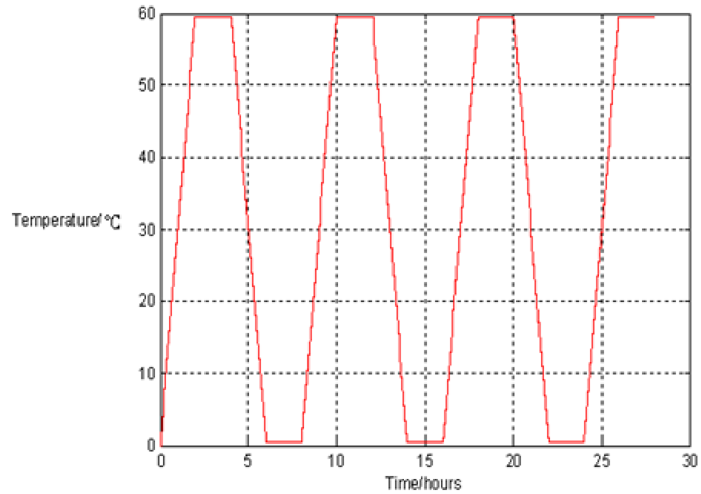

Figure 2. Ambient Temperature Profile

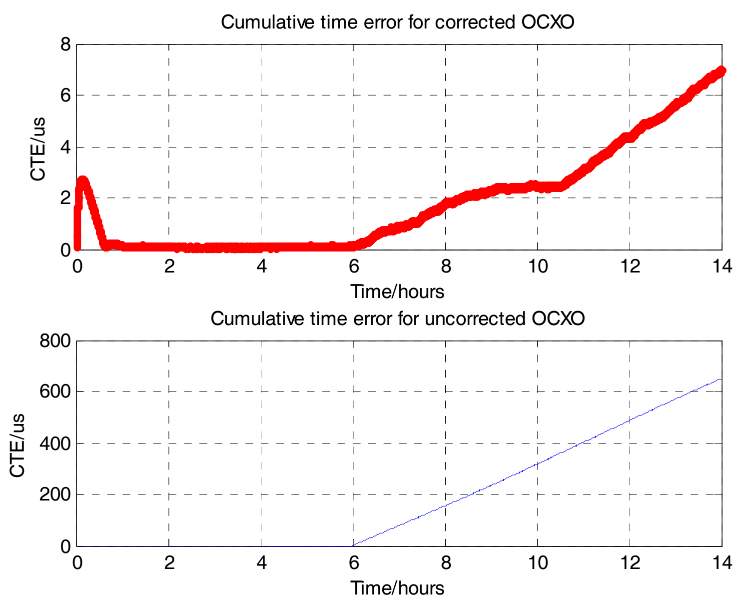

Figure 3. CTE for corrected and uncorrected OCXO during locked and holdover mode. Holdover initiated at 6 hours.

Other papers such as [2] [4] [5] [6] [7] have used a more direct modeling approach for the parameter identification. Equation (20) is a model created through this more direct modeling approach. Here the correction signal is directly related to temperature and ageing and does not take into consideration the control circuitry implementation as in Equation (17).

$$y(k) = a * u^2(k) + b * u(k) + c + d * k + v(k) \quad (20)$$

A Recursive Least Squares method can be used to identify the parameters of this model. Simulation results show that the performance of the model of Equation (20) is not as good as the model of Equation (17). Figure 4 shows the comparison results. We run 100 simulations and the maximum CTE for Equation (17) and Equation

(20) are compared. In Figure 4, the dashed line represents the CTE for the model of Equation (20) and the solid line represents the CTE for the model of Equation (17). In the remainder of the paper, we call the model of Equation (17) the model that includes the control loop and the model of Equation (20) is called the direct model. The model that includes the control loop has better performance than the direct model. The reason is that the correction signal in locked mode is generated by the control loop. Therefore, the direct model, which omits the control loop, may produce errors in determining the correction signal in holdover mode. The model that includes the control loop more precisely captures how the correction signal is created in locked mode.

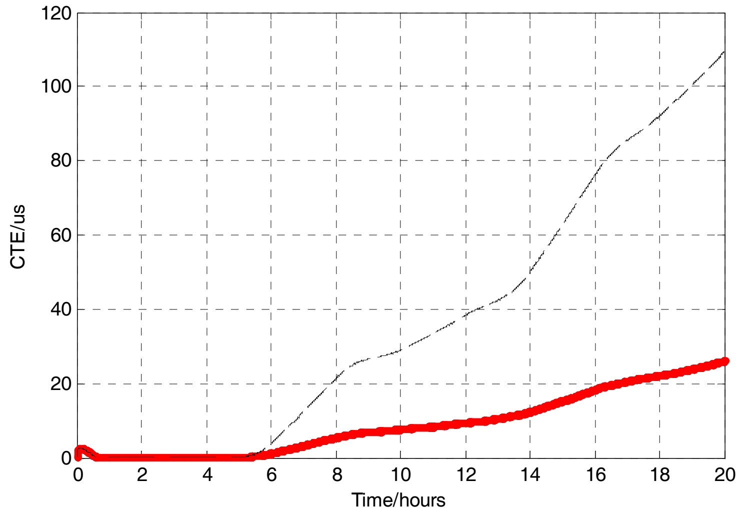

Figure 4. CTE for direct model of Equation (20) and more complex model of Equation (17). Holdover initiated at 5 hours.

5. Cumulative Time Error Upperbound

A problem for wireless network providers is that they want to know the holdover worst case scenario. Therefore, we investigate the analytical CTE upperbound of the timing module. The first step is to identify the distribution of the parameter estimates. According to Equation (17), there are 5 parameters which need to be estimated. However, there are only 4 parameters in Equation (16). The parameter e in Equation (17) is the noise parameter, which is not used in estimating the correction signal. We only need the parameter estimates $\hat{a}, \hat{b}, \hat{c}$ and $\hat{d}$ to create the correction signal for compensating the oscillator. Hence, in the remainder of this paper, we set $\theta_0 = [a \;\; b \;\; c \;\; d]^T$ and $\hat{\theta} = \left[\hat{a} \;\; \hat{b} \;\; \hat{c} \;\; \hat{d}\right]^T$. Through analyzing θ_0 and $\hat{\theta}$, the characteristics of the parameter estimates can be obtained. According to [8], the parameter estimates vector $\hat{\theta}$ has a Gaussian joint distribution with mean value θ_0, where θ_0 is the true parameter value, and covariance matrix P_N which is given as,

$$\hat{\theta} - \theta_0 \in N(0, P_N) \tag{21}$$

Since P_N is the covariance matrix of the joint distribution of vector $\hat{\theta} - \theta_0$, the covariance and correlation between the different components of $\hat{\theta} - \theta_0$ can be obtained. Hence, we know that

$$\left(\hat{\theta} - \theta_0\right)^T P_N^{-1}(\hat{\theta} - \theta_0) \in \chi^2(d) \tag{22}$$

Equation (22) is a direct application of the definition of the χ^2 distribution. The probability of $|\hat{\theta} - \theta_0|^2_{P_N^{-1}}$ can be represented by $P(|\hat{\theta} - \theta_0|^2_{P_N^{-1}})$. Hence, by checking the χ^2 statistical table, we know

$$P\left(|\hat{\theta} - \theta_0|^2_{P_N^{-1}}\right) = P\left(\left(\hat{\theta} - \theta_0\right)^T P_N^{-1}(\hat{\theta} - \theta_0)\right) = 95\%$$

when $\left(\hat{\theta} - \theta_0\right)^T P_N^{-1}\left(\hat{\theta} - \theta_0\right) \le 9.49$, because the degree of freedom of the χ^2 distribution is 4 [9].

The estimate of the oscillator frequency stability can be approximated as,

$$\hat{y}(t) = \hat{a} \cdot u^2(t) + \hat{b} \cdot u(t) + \hat{c} + \hat{d} \cdot t \tag{23}$$

Hence, the cumulative time error is

$$CTE = |\sum_{i=1}^{N}(\hat{y}(t_i) - y(t_i))| \quad (24)$$

The CTE 95% probability upperbound is the maximum value of CTE subject to $(\hat{\theta} - \theta_0)^T P_N^{-1}(\hat{\theta} - \theta_0) \leq 9.49$.

$$\mathrm{CTE_{max}} = \max_{\hat{\theta}} \left| \sum_{i=1}^{N} (\hat{y}(t_i) - y(t_i)) \right|$$
$$such\ that\ (\hat{\theta} - \theta_0)^T P_N^{-1}(\hat{\theta} - \theta_0) \leq 9.49 \quad (25)$$

An eigenvector method is used to solve Equation (25). First, the column vectors $Z = \hat{\theta} - \theta_0$ and $R = [\sum_{i=1}^{N} x^2(t_i) \ \ \sum_{i=1}^{N} x(t_i) \ \ N \ \ \sum_{i=1}^{N} t_i]^T$ are defined. The problem of finding the 95% maximum value of $|\sum_{i=1}^{N}(\hat{y}(t_i) - y(t_i))|$ is equivalent to Equation (26).

$$\max_{\hat{\theta}} \left(\sum_{i=1}^{N} (\hat{y}(t_i) - y(t_i)) \right)^2 = max(Z^T * R)^2$$
$$= max(Z^T * (R * R^T) * Z)$$
$$such\ that\ Z^T P_N^{-1} Z \leq 9.49 \quad (26)$$

We set $PI = P_N^{-1}$. The generalized eigenvalue problem of $R * R^T$ can be solved by Equation (27).

$$R * R^T * V = PI * V * D \quad (27)$$

The matrix *D* is a diagonal matrix with the generalized eigenvalues of $R * R^T$ on the main diagonal. The matrix *V* is a full matrix whose columns are the corresponding eigenvectors of *D*. The maximum value of the elements on *D*'s main diagonal is denoted h, and the corresponding index is denoted k. Let v_k denote the *k-th* column of *V*, which corresponds to the maximum eigenvalue *h*. From Equation (27), we get

$$R * R^T * v_k = h * PI * v_k \quad (28)$$

Equation (28) multiplied by ${v_k}^T$ on the left side gives

$${v_k}^T * R * R^T * v_k = {v_k}^T * h * PI * v_k \quad (29)$$

Z is calculated as follows:

$$Z = \sqrt{\frac{9.49}{{v_k}' * PI * v_k}} * v_k \quad (30)$$

Thus,

$$max \left(\sum_{i=1}^{N} (\hat{y}(t_i) - y(t_i)) \right)^2 = max(Z^T * R * R^T * Z)$$

$$= \sqrt{\frac{9.49}{{v_k}' * PI * v_k}} * {v_k}' * R * R'$$
$$* \sqrt{\frac{9.49}{{v_k}' * PI * v_k}} * v_k$$
$$= \frac{9.49}{{v_k}' * PI * v_k} * {v_k}' * R * R' * v_k$$
$$= \frac{9.49}{{v_k}' * PI * v_k} * {v_k}' * PI * v_k * h$$
$$= 9.49 * h \quad (31)$$

Therefore, the 95% maximum cumulative time error can be obtained by computing the square root of the maximum $|CTE|^2$ when $\hat{\theta}$ is located on the 95% probability confidence ellipsoid boundary. This maximum CTE is our analytical 95% probability CTE upperbound.

We use the Monte Carlo simulation method to verify this analytical 95% CTE upperbound [10]. Figure 5 shows the comparison among 95% probability analytical CTE upperbound, Monte Carlo maximum CTE upperbound, and Monte Carlo 95% probability CTE upperbound. In the simulation, 100 simulations are run. The 5^{th} maximum CTE of 100 simulations is used to represent the Monte Carlo 95% probability CTE upperbound and the maximum CTE of 100 simulations to represent the Monte Carlo maximum CTE upperbound. The analytical upperbound of the CTE actually lies between the maximum CTE and the 95% upperbound of CTE. The reason is that a $\hat{\theta}$ which is located outside the 95% probability confidence ellipsoid does not always result in a larger CTE than all $\hat{\theta}$ in the 95% probability confidence ellipsoid.

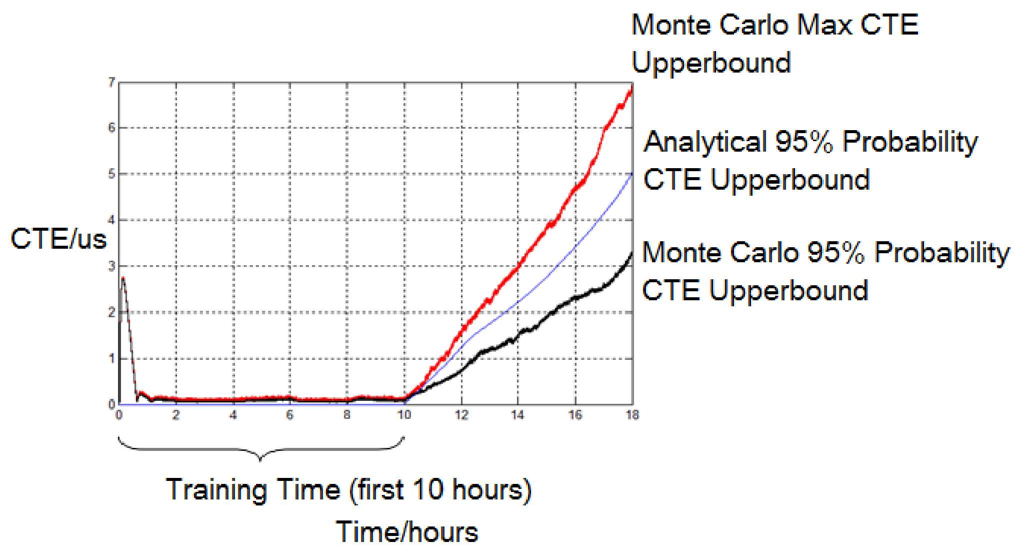

Figure 5. Comparison Result between Analytical CTE Upperbound and Monte Carlo CTE Upperbound

6. Conclusions

In this paper, an adaptive control algorithm is introduced to enhance the frequency stability of OCXO in timing modules of base stations. A model which includes the control loop is created and the Recursive Prediction Error Method (RPEM) is used to identify the parameters. The simulation results show that this method provides better performance of the oscillator than the uncorrected oscillator and the oscillator corrected using a direct model proposed in the previously published literature. The analytical oscillator cumulative time error in holdover mode is investigated and a good result is obtained. The 95% maximum error bound in holdover mode for the oscillator is determined analytically and in comparison to the Monte Carlo Method.

References

[1]. “Recommended Minimum Performance Standards for cdma 2000 Spread Spectrum Base Stations,”3GPP2 Standard C.S0010-C, release C, version 2, release data February 24, 2006.

[2]. C.W.T. Nicholls and P. Wu, “Ultra Low Cost Base Station Timing Module”, Proceedings of the IEEE International Frequency Control Symposium and Exposition, pp. 1318-1323, 2007.

[3] L. Ljung and T. Söderström, "Theory and Practice of Recursive Identification", MIT Press, 1983. ISBN-10: 026212095X

[4] B.M. Penrod, “Adaptive Temperature Compensation of GPS Disciplined Quartz and Rubidium Oscillators”, Proceedings of the IEEE International Frequency Control Symposium, pp. 980 – 987, 1996

[5] S.R. Stein, “Kalman Filter Analysis of Precision Clocks with Real-Time Parameter Estimation”, Proceedings of the 43rd Annual Symposium on Frequency Control, pp. 232-236, 1989.

[6] W. Su and R.L. Filler, “A New Approach to Clock Modeling and Kalman Filter Time and Frequency Prediction”, Proceedings of the IEEE International Frequency Control Symposium, pp. 331-334, 1993.

[7] C.W.T. Nicholls and G.C. Carleton, “Adaptive OCXO Drift Correction Algorithm”, Proceedings of the IEEE International Frequency Control Symposium and Exposition, pp. 509 – 517, 2004.

[8] L. Ljung, “System Identification: Theory for the User”, Prentice Hall PTR, 1999. ISBN-10: 0136566952

[9] χ^2statistics table from http://home.comcast.net/~sharov/PopEcol/tables/chisq.html (accessed October 5, 2009).

[10] I. Manno, “Introduction to the Monte Carlo Method”, Akademiai Kiado Press, 1999. ISBN-10: 9630576155